



HAL
open science

Disparity Map Estimation Using A Total Variation Bound

Wided Miled, Jean-Christophe Pesquet, Michel Null Parent

► **To cite this version:**

Wided Miled, Jean-Christophe Pesquet, Michel Null Parent. Disparity Map Estimation Using A Total Variation Bound. Third Canadian Conference on Computer and Robot Vision, Jun 2006, Quebec. inria-00001255

HAL Id: inria-00001255

<https://inria.hal.science/inria-00001255>

Submitted on 14 Apr 2006

HAL is a multi-disciplinary open access archive for the deposit and dissemination of scientific research documents, whether they are published or not. The documents may come from teaching and research institutions in France or abroad, or from public or private research centers.

L'archive ouverte pluridisciplinaire **HAL**, est destinée au dépôt et à la diffusion de documents scientifiques de niveau recherche, publiés ou non, émanant des établissements d'enseignement et de recherche français ou étrangers, des laboratoires publics ou privés.

Disparity Map Estimation Using A Total Variation Bound

Wided Miled^{1,2}, Jean Christophe Pesquet² and Michel Parent¹

¹INRIA, IMARA Project
Domaine de Voluceau
78150 Le Chesnay, Cedex France
email : {wided.miled,michel.parent}@inria.fr

²Institut Gaspard Monge / UMR-CNRS 8049
Université Marne-la-Vallée
77454 Champs-sur-Marne, France
e-mail: pesquet@univ-mlv.fr

Abstract

This paper describes a new variational method for estimating disparity from stereo images. The stereo matching problem is formulated as a convex programming problem in which an objective function is minimized under various constraints modelling prior knowledge and observed information. The algorithm proposed to solve this problem has a block-iterative structure which allows a wide range of constraints to be easily incorporated, possibly taking advantage of parallel computing architectures. In this work, we use a Total Variation bound as a regularization constraint, which is shown to be well-suited to disparity maps. Experimental results for standard data sets are presented to illustrate the capabilities of the proposed disparity estimation technique.

1. Introduction

Stereo vision systems determine depth information from a pair of left and right images which are taken at the same time, but from slightly different viewpoints. The most important problem in stereo image processing is to find corresponding pixels from both images, leading to the so-called disparity estimation. A number of studies have been reported on the disparity estimation problem since the 1970's [1] including feature-based, area-based and energy-based approaches. The feature-based approach extracts features from image pairs (e.g., edges, lines, corners) and then establishes correspondence between these features. They yield accurate information but the main drawback of the method is the sparseness of the recovered depth map. The area-based approach finds corresponding points by measuring similarity based on window correlation. This approach attempts to determine the correspondence for every pixel,

which results in a dense depth map, but tends to fail at depth discontinuities and low textured areas. Many attempts have been made to remedy this serious problem by making the size and shape of the matching window adaptive to the local variation of disparity characteristics [2], [3], [4]. Energy-based approaches attempt to overcome this problem by minimizing variational formulations, where a data term and a smoothness term are penalized. An excellent survey on dense stereo methods can be found in [5].

Variational approaches were introduced in image processing for restoration and denoising problems and have subsequently attracted much interest in the computer vision community where they were first devised for the purpose of estimating optical flow from a sequence of images. Numerical studies on optical flow via variational techniques have been performed in the last decade. For a review, the reader can refer to [6]. These studies showed that the variational optical flow methods are among the most powerful techniques, which naturally motivates their extension for disparity map estimation [7], [8].

Variational methods are based on the minimization of an energy functional $E(u)$ which consists of a data term and a regularization term

$$E(u) = E_{\text{data}}(u) + \lambda E_{\text{smooth}}(u), \quad (1)$$

where u denotes the field to be estimated and λ is a positive coefficient that weights the smoothness term relatively to the first data term. This functional is often minimized via an iterative procedure derived from the associated non-linear Euler-Lagrange equations. This allows to prove, in many cases, the existence and uniqueness of the optimal solution but requires the implementation of sophisticated numerical schemes [7]. Moreover, the discretization of the PDE is a delicate problem and the choice of the Lagrange parameter λ is a difficult task. The latter problem becomes even more

involved when a sum of regularization terms has to be considered to address multiple constraints which may arise in the problem.

The aim of this study is to propose a novel variational method for disparity map estimation based on the set theoretic approach. This approach uses a criterion of feasibility rather than a penalized optimality criterion. Then, a solution is acceptable if it is consistent with all available information arising from the prior knowledge and the observed data. Each piece of information is represented by a convex set and the feasibility set, that is the intersection of these sets, represents all acceptable solutions. One of the advantages of this approach is that it is often easier to define the constraint sets than to choose the optimal values of the Lagrange parameters in a regularization method.

The most popular method that involves the set theoretic formulation is the Projection Onto Convex Sets (POCS). Typically, this iterative method successively projects partial solutions onto property sets. POCS is one of the most prevalent tool for solving recovery problems in image processing and it has also been used for the restoration of the optical flow [9]. However, this method presents several shortcomings, including its slow convergence and the fact that it is not well suited for an implementation on parallel processors. Numerous approaches have been developed in order to overcome the above limitations. The reader is referred to [10] for a review of existing projection techniques.

The basic principle of the approach proposed in this work is to formulate the matching problem as a convex programming problem. More precisely, a quadratic objective function is minimized under certain constraints and the resulting optimization problem is solved via a block-iterative parallel decomposition method. This method allows a wide range of constraints to be easily incorporated, thus leading to improved results. We propose in this work to use the Total Variation as a regularizing constraint. As shown in the seminal work of [11], the main advantage of this regularity measure is that it preserves the edges in the image while smoothing the homogeneous areas. It is therefore appropriate for disparity maps that often contain large homogeneous regions.

Our paper is organized as follows. Section 2 describes the binocular vision system and defines our stereo model. In Section 3, we introduce the mathematical background and necessary notations for the method proposed in this paper. Then we present the set theoretic disparity map estimation and describe the constraints we incorporate in the problem in Section 4. Experiment results are presented in Section 5, followed by a conclusion in Section 6.

2. Problem statement

In this section, we formulate the matching problem and describe our stereo model.

2.1. Stereo vision system

The considered stereo vision system consists of two cameras positioned side by side in order to obtain left and right images. The cameras are separated by a fixed distance T , called baseline, and should have the same focal length f . For each pixel in the left image, a corresponding pixel is matched in the right image. The camera geometry can significantly affect the amount of processing required by the matching strategy. We consider the parallel camera configuration, so that both cameras are located on a horizontal plane and have parallel optical axes.

A constraint that is often considered in stereo vision systems is the epipolar geometry constraint. This constraint involves that any point lying on an epipolar line in one image necessarily corresponds to a point lying on the homologous epipolar line in the other image. When the cameras are parallel, as we have assumed here, the epipolar lines are horizontal as shown in Figure 1. Although sometimes convergent cameras are used, suitable algorithms, such as the one described in [12], can be applied to rectify the images. Consequently, whether the cameras are parallel or rectification is applied, the vertical component of the disparity vector vanishes, so that only a scalar value has to be estimated.

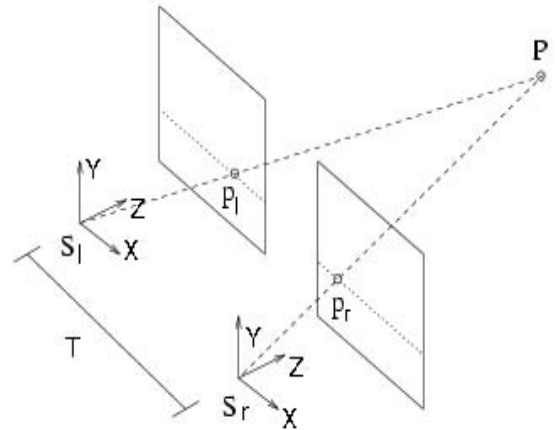


Figure 1. Epipolar geometry within a parallel camera configuration.

Let I_l and I_r be the left and right views of a stereo pair, respectively. Two points $p_l = (x_l, y_l)$ and $p_r = (x_r, y_r)$ in the images I_l and I_r are said to be matched if and only

if they are the projection of the same 3-D point on the two image planes. In this case, the disparity u pointing from p_l to p_r is given by $u = x_l - x_r$.

2.2. Stereo model

A disparity value for each pixel of an image is estimated by searching a corresponding point in the other image. Each possible corresponding point, designated as a candidate, is evaluated using a cost function. The sum of squared intensity differences (SSD) is commonly used as the similarity measure due to its simplicity:

$$\tilde{J}(u) = \sum_{(x,y) \in \mathcal{D}} [I_l(x,y) - I_r(x-u,y)]^2, \quad (2)$$

where $\mathcal{D} \subset \mathbb{N}^2$ is the image support. In order to simplify the notations, we have not made explicit that u is a function of (x,y) in the above expression. Given a set \mathcal{A} of admissible candidate disparity vectors, an optimal disparity field \hat{u} is given by

$$\hat{u} = \arg \min_{u \in \mathcal{A}} \tilde{J}(u). \quad (3)$$

Assuming that an initial disparity estimate \bar{u} of u is available, for example from a previous estimation (possibly within an iterative process) and that the magnitude difference of the fields \hat{u} and \bar{u} is relatively small, we can approximate the warped right image around \bar{u} by a Taylor expansion as follows:

$$I_r(x-u,y) \simeq I_r(x-\bar{u},y) - I_r^x(x-\bar{u},y)(u-\bar{u}), \quad (4)$$

where $I_r^x(x-\bar{u},y)$ is the horizontal gradient of the warped right image.

Introducing the notations:

$$L(x,y) = I_r^x(x-\bar{u},y), \quad (5)$$

and

$$r(x,y) = -I_l(x,y) + I_r(x-\bar{u},y) + \bar{u} L(x,y), \quad (6)$$

we end up with the following quadratic criterion, related to the linearized model (4):

$$J(u) = \sum_{(x,y) \in \mathcal{D}} [L(x,y)u - r(x,y)]^2. \quad (7)$$

Now, our purpose is to recover the true disparity image u from the observed fields L and r . This problem is ill-posed and it must therefore be regularized by adding some constraints to the solution. Appropriate convex constraints will be subsequently defined so as to formulate the problem within the framework which is described in the next section.

3. Convex set theoretic framework

3.1. Formulation of inverse problems

Many problems in image processing have been successfully addressed from a set theoretic formulation. In the existing works, the main concern is to find solutions that are consistent with all information arising from prior knowledge and the observed data. Every known property is represented by a set in the solution space and the intersection of these sets constitutes the family of acceptable solutions. In many problems, the aim is to find an acceptable solution u minimizing a certain cost function [10]. A general formulation of this problem in a Hilbert image space \mathcal{H} is

$$\min_{u \in \mathcal{H}} J(u) \text{ subject to constraints } (\Psi_i)_{1 \leq i \leq m}, \quad (8)$$

where $J : \mathcal{H} \rightarrow]-\infty, +\infty]$ represents the objective function to be minimized and the constraints $(\Psi_i)_{1 \leq i \leq m}$ arise from the available information. A family of property sets of \mathcal{H} can be constructed as follows

$$\forall i \in \{1, \dots, m\}, \quad S_i = \{u \in \mathcal{H} \mid u \text{ satisfies } \Psi_i\}. \quad (9)$$

Thus S_i is the set of all estimates that are consistent with the constraint Ψ_i . The solution set consisting of solutions that are consistent with all available information is the feasibility set

$$S = \bigcap_{i=1}^m S_i. \quad (10)$$

Restricting our study to convex feasibility problems, a general formulation is therefore

$$\text{Find } u \in S = \bigcap_{i=1}^m S_i \text{ such that } J(u) = \inf J(S), \quad (11)$$

where the objective J is a convex function and the constraints sets $(S_i)_{1 \leq i \leq m}$ are closed convex subsets of \mathcal{H} . It is more convenient to model the constraint sets $(S_i)_{1 \leq i \leq m}$ as level sets:

$$\forall i \in \{1, \dots, m\}, \quad S_i = \{u \in \mathcal{H} \mid f_i(u) \leq \psi_i\}, \quad (12)$$

where $(f_i)_{1 \leq i \leq m}$ are continuous convex functions and $(\psi_i)_{1 \leq i \leq m}$ are real parameters. We assume that the problem is consistent, i.e. $S \neq \emptyset$.

3.2. Subgradient projections

Here, we briefly recall the basic facts on subgradient projections which are necessary for our problem. More details can be found in [13]. The image space is a real Hilbert

space \mathcal{H} with scalar product $\langle \cdot | \cdot \rangle$ and norm $\| \cdot \|$. A vector $t \in \mathcal{H}$ is a subgradient of a continuous convex function $f : \mathcal{H} \rightarrow \mathbb{R}$ at $u \in \mathcal{H}$ if

$$\forall v \in \mathcal{H}, \quad \langle v - u | t \rangle + f(u) \leq f(v). \quad (13)$$

(As f is continuous, it always possesses at least one subgradient at each point u .) The set of all subgradients of f at u is the subdifferential of f at u and is denoted by $\partial f(u)$. If f is differentiable at u , then $\partial f(u) = \{\nabla f(u)\}$.

Let $\psi \in \mathbb{R}$ and $C = \{v \in \mathcal{H} \mid f(v) \leq \psi\}$ be a nonempty closed and convex subset of \mathcal{H} . Fix $u \in \mathcal{H}$ and a subgradient $t \in \partial f(u)$, the subgradient projection $P_C u$ of u onto C is given by:

$$P_C u = \begin{cases} u - \frac{f(u) - \psi}{\|t\|^2} t, & \text{if } f(u) > \psi; \\ u, & \text{if } f(u) \leq \psi. \end{cases} \quad (14)$$

We note that computing $P_C u$ is often a much easier task than computing the exact projection onto C , as the latter amounts to solving a constrained minimization problem [13]. However, when the projection is easy to compute, one can use it as a subgradient projection.

3.3. An efficient algorithm

We now proceed to the description of the quadratic programming algorithm developed in [13] to solve the quadratic convex problem (11) which is equivalent to minimizing

$$u \mapsto \langle u - u_0, R(u - u_0) \rangle \quad (15)$$

over S , when R is a self-adjoint definite positive operator and $u_0 \in \mathcal{H}$.

3.3.1 Algorithm

1. Fix $\varepsilon \in]0, 1/m[$ and set $n = 0$.
2. Take a nonempty index set $I_n \subseteq \{1, \dots, m\}$.
3. For every $i \in I_n$, set $a_{i,n} = P_{i,n} - u_n$ where $P_{i,n}$ is a subgradient projection of u_n onto S_i as in (14).
4. Choose weights $\{\xi_{i,n}\}_{i \in I_n} \subset]\varepsilon, 1]$ such that $\sum_{i \in I_n} \xi_{i,n} = 1$. Set $v_n = \sum_{i \in I_n} \xi_{i,n} a_{i,n}$ and $L_n = \sum_{i \in I_n} \xi_{i,n} \|a_{i,n}\|^2$.
5. If $L_n = 0$, exit iteration. Otherwise, set $b_n = u_0 - u_n$, $c_n = R b_n$, $d_n = R^{-1} v_n$ and $\tilde{L}_n = L_n / \langle d_n, v_n \rangle$.
6. Choose $\lambda_n \in [\varepsilon \tilde{L}_n, \tilde{L}_n]$ and set $d_n = \lambda_n d_n$.
7. Set $\pi_n = -\langle c_n, d_n \rangle$, $\mu_n = \langle b_n, c_n \rangle$, $\nu_n = \lambda_n \langle d_n, v_n \rangle$ and $\rho_n = \mu_n \nu_n - \pi_n^2$.

8. Set

$$u_{n+1} = \begin{cases} u_n + d_n, & \text{if } \rho_n = 0, \pi_n \geq 0; \\ u_0 + (1 + \frac{\pi_n}{\nu_n}) d_n, & \text{if } \rho_n > 0, \pi_n \nu_n \geq \rho_n; \\ u_n + \frac{\nu_n}{\rho_n} (\pi_n b_n + \mu_n d_n), & \text{if } \rho_n > 0, \pi_n \nu_n < \rho_n. \end{cases}$$

9. Set $n = n + 1$ and go to step 2.

In [13], it has been shown that the algorithm offers a lot of flexibility in terms of implementation. In particular, several processors can be used in parallel to compute the subgradient projections on the different constraint sets $(S_i)_{1 \leq i \leq m}$, leading to improved results while reducing the computational time.

4. Disparity estimation

We now come back to the problem of disparity estimation exploiting the convex set theoretic framework described in Section 3. Two basic elements are required to solve this problem:

1. A data formation model, i.e., an objective function J to be minimized.
2. Convex constraints arising from prior information and yielding closed and convex property sets $(S_i)_{1 \leq i \leq m}$.

4.1. Energy function

The objective function is the quadratic measure deduced from our linearized data formulation (see Section 2). This function models the assumption of a constant intensity value in both views. However, for occlusion points that are visible on only one of the two stereo images, this assumption is no longer valid. These points are considered as deviating data points (outliers) and have, therefore, to be detected and discarded from the summation of pixel matching cost in equation (7). Here, we exploit the uniqueness and ordering constraints to detect the presence of occlusions. For a review of some existing occlusion detection methods, the reader is referred to [14].

Moreover, since $L(x, y)$ in (7) may be zero, we introduce the additive term $\alpha \|u - \bar{u}\|^2$ to make J strictly convex, in compliance with the assumption required to guarantee the convergence of the proposed algorithm [13]. Denoting \mathcal{O} the occlusion field and $\mathbf{x} = (x, y)$ a point in the left view, the resulting objective criterion is given by:

$$J(u) = \sum_{\mathbf{x} \in \mathcal{D} \setminus \mathcal{O}} [L(\mathbf{x}) u(\mathbf{x}) - r(\mathbf{x})]^2 + \alpha \sum_{\mathbf{x} \in \mathcal{D}} [u(\mathbf{x}) - \bar{u}(\mathbf{x})]^2, \quad (16)$$

where \bar{u} is an initial estimate and α is a positive constant that weights the first term relatively to the second.

In order to render the approach more robust with respect to outliers, the additive term has to handle with the occlusion problem. It is therefore important to deal with a consistent initial disparity field. In our case, we consider an initialization derived from the left-right consistency constraint. More precisely, using a correlation based method, we compute left-to-right and right-to-left initial disparity maps, denoted respectively by \bar{u}_l and \bar{u}_r , and for each point $\mathbf{x} = (x, y)$ we take $\bar{u}(\mathbf{x}) = \bar{u}_r(x - \bar{u}_l(\mathbf{x}), y)$. We then iteratively refine the initial disparity estimate by choosing the result from a previous estimate as the initial value of the next step. There are two advantages of using this iterative procedure. Firstly, it improves the quality of the solution. The second advantage is that it reduces the dependence of the final solution on the initial estimate \bar{u} .

Finally, we note that minimizing the functional (16) is obviously equivalent to minimizing (15) where $R = L^*L + \alpha \text{Id}$ and $u_0 = R^{-1}(L^*r + \alpha\bar{u})$ (here, L denotes the diagonal operator $u \mapsto (L(\mathbf{x})u(\mathbf{x}))_{\mathbf{x}}$ and L^* is its adjoint). It can be noticed that the operator R is diagonal in our problem, which facilitates the implementation of the algorithm.

4.2. Convex constraints

The construction of convex property sets is based on the various properties of the field to be estimated. In most stereo vision applications, the disparity map should be smooth in homogeneous areas while keeping sharp edges. This can be achieved with the help of a suitable regularization constraint. It is well-known that using the *Tikhonov* regularization, by considering a quadratic term, often introduces too much regularization, resulting in oversmoothed edges. We address this problem by using the Total Variation (TV) regularization constraint. Initially introduced by Rudin, Osher and Fatemi [11], this regularity measure has already proven to be very powerful in image recovery and denoising problems [15], [16] which motivates its extension to the field of variational stereo methods [6], [8]. For a differentiable analog image defined on a domain Ω , the TV is given by

$$\text{TV}(u) = \int_{\Omega} |\nabla u(x, y)|_2 \, dx \, dy, \quad (17)$$

where ∇u is the gradient of u . In digital applications, images are discretized on a finite $N \times M$ sampling grid. The Total Variation of a digital image $u = (u^{i,j})_{0 \leq i, j \leq N-1, M-1}$ is obtained by discretizing (17),

yielding

$$\begin{aligned} \text{TV}(u) = & \sum_{i=0}^{N-2} \sum_{j=0}^{M-2} \sqrt{|u^{i+1,j} - u^{i,j}|^2 + |u^{i,j+1} - u^{i,j}|^2} \\ & + \sum_{i=0}^{N-2} |u^{i+1,M-1} - u^{i,M-1}| \\ & + \sum_{j=0}^{M-2} |u^{N-1,j+1} - u^{N-1,j}|. \end{aligned} \quad (18)$$

Practically, $\text{TV}(u)$ measures the amount of oscillations in the image u . Hence, if u is known a priori to have a certain level of oscillation so that a bound τ is available on the total variation, controlling $\text{TV}(u)$ restricts the solutions to the convex set

$$S_1 = \{u \in \mathcal{H} \mid \text{TV}(u) \leq \tau\}. \quad (19)$$

The expression of a subgradient projection P_1 onto S_1 is given in [16]. It should be noted that $\text{TV}(u)$ constitutes a geometrical feature that can be estimated from experiments and image databases for a same class of images. Moreover, it has been shown in [16] that this constrained based method is robust with respect to the choice of the bound τ .

Many other additional constraints on the original image may be used. An example of possible prior knowledge is the range of disparity values. Given a set of candidate disparity vectors, we can impose minimal and maximal amplitudes, denoted respectively by u_{\min} and u_{\max} , on the amount of allowed disparity. The set associated with this information is

$$S_2 = \{u \in \mathcal{H} \mid u_{\min} \leq u \leq u_{\max}\}. \quad (20)$$

We note that in practice u_{\min} and u_{\max} are often available.

Finally, we use another constraint inspired from the work in [7] that uses a regularization term $(\nabla u)^\top D(\nabla I_l)(\nabla u)$ based on the Nagel-Enkelmann operator [17]. The main idea of this constraint is that discontinuities in the disparity map are preserved accordingly to the edges of the left image I_l . Thus, the constraint has an isotropic behavior within uniform areas, but at object edges it introduces an anisotropic smoothing. Details given in [7] about this oriented smoothness constraint can help for giving an approximation κ of this regularization term leading to the following convex set

$$S_3 = \{u \in \mathcal{H} \mid (\nabla u)^\top D(\nabla I_l)(\nabla u) \leq \kappa\}. \quad (21)$$

We remark that the exact projection onto S_2 is straightforwardly obtained whereas a subgradient projection onto S_3 can be easily calculated.

In summary, we formulate the corresponding problem as the minimization of (16) on $S = \bigcap_{i=1}^3 S_i$, where the sets $(S_i)_{1 \leq i \leq 3}$ are given by equations (19), (20) and (21).

5. Experimental results

In this section, we evaluate the benefits which can be drawn from our approach using four standard data sets from the Middlebury database [5], named *Tsukuba*, *Sawtooth*, *Venus* and *Map*. For all experiments, the parameter α in equation (16) was set to 50, which ensures a good trade-off between convergence speed and estimation accuracy. We note that values ranging from 10 to 100 also lead to reliable results. A value of 10^4 for the total variation bound τ was found to be appropriate for the considered data set of test images.

The evaluation measure is the Average Absolute Disparity Error (AADE) between estimated u_e and ground truth disparities u_t :

$$\text{AADE} = \frac{1}{N \times M} \sum_{(x,y)} |u_t(x,y) - u_e(x,y)|, \quad (22)$$

where $N \times M$ is the total number of pixels. The error criterion is measured through different areas in the image, classified as untextured (B_{untext}), discontinuous (B_{disc}) and the entire image (B_{all}). Following the evaluation procedure in [5], only non-occluded pixels are considered in all three cases.

The quantitative results in Table 1 and the extracted disparity maps in Figure 3 demonstrate the high quality performance of our approach. The observed improvements demonstrate the ability of the algorithm to compute smooth disparity maps with accurate depth discontinuities in a wide variety of situations. This is a consequence of using the Total Variation constraint. Furthermore, Figure 2 shows the comparison of recovered occlusion maps with ground truth ones. Our results are very close to the ground truth occlusion maps which proves that our method can efficiently handle the uniqueness and ordering constraints for about all visible pixels.

For comparison purposes, the results obtained from other dense stereo algorithms, available at <http://www.middlebury.edu/stereo> and having the top rank in the online evaluation on the same website, are also included in Table 1. This comparison shows that our approach is quite competitive with state-of-the-art methods.

In addition, Table 2 reports the error values, on all non-occluded image pixels, obtained when one of the constraints (either S_1 or S_3) is missing. This confirms that it is useful to incorporate multiple constraints.

6. Conclusion

In this paper, we have introduced a convex set theoretic formulation for the estimation of the disparity map from a

stereo pair. The resulting optimization problem is solved via a block iterative parallel decomposition method. This efficient algorithm allowed us to combine a Total Variation constraint with additional convex constraints so as to smooth homogeneous regions while preserving discontinuities. Experiments on various data sets demonstrate that the performance of the proposed approach is comparable with state-of-the-art methods. In our future work, we will continue to investigate the set theoretic framework that provides a new perspective for matching problems while leading to efficient numerical solutions.

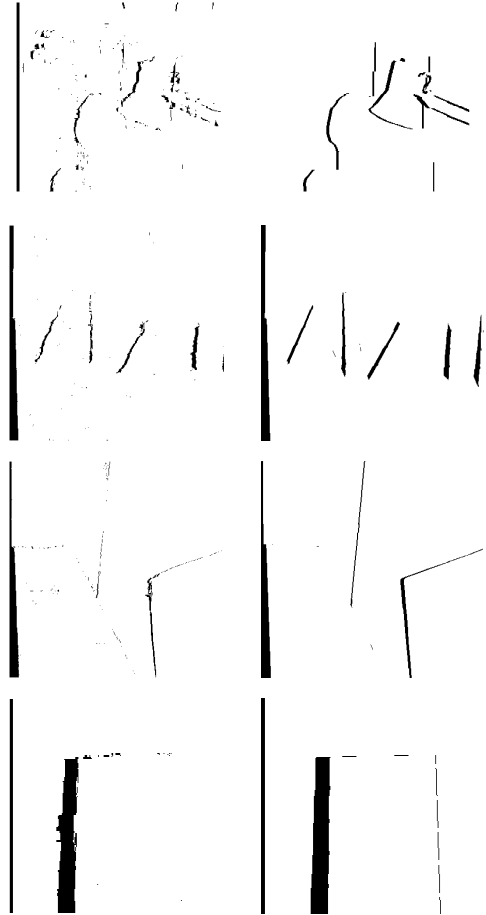


Figure 2. Occlusion maps for the Middlebury stereo data. Left column: our results. Right column: ground truth.

References

- [1] D. Marr and T. Poggio. Cooperative computational of stereo disparity. *Science*, 194:209–236, 1976.

| Technique | Tsukuba | | | Sawtooth | | | Venus | | | Map | |
|----------------------|-------------|--------------|-------------|-------------|--------------|-------------|-------------|--------------|-------------|-------------|-------------|
| | B_{all} | B_{untext} | B_{disc} | B_{all} | B_{untext} | B_{disc} | B_{all} | B_{untext} | B_{disc} | B_{all} | B_{disc} |
| Segm.+glob.vis. [18] | 0.18 | 0.17 | 0.47 | 0.24 | 0.19 | 0.40 | 0.31 | 0.31 | 0.52 | 0.67 | 3.45 |
| Graph+segm. [19] | 0.15 | 0.09 | 0.49 | 0.24 | 0.19 | 0.38 | 0.26 | 0.27 | 0.37 | 0.81 | 4.4 |
| 2-pass DP [20] | 0.28 | 0.34 | 0.57 | 0.25 | 0.20 | 0.53 | 0.30 | 0.33 | 0.53 | 0.37 | 2.81 |
| Patch-based [21] | 0.12 | 0.12 | 0.32 | 0.23 | 0.18 | 0.43 | 0.27 | 0.29 | 0.35 | 0.39 | 1.15 |
| Proposed | 0.29 | 0.24 | 0.51 | 0.23 | 0.19 | 0.41 | 0.24 | 0.26 | 0.39 | 0.35 | 1.27 |

Table 1. Performance comparison of stereo algorithms using the AADE measure.

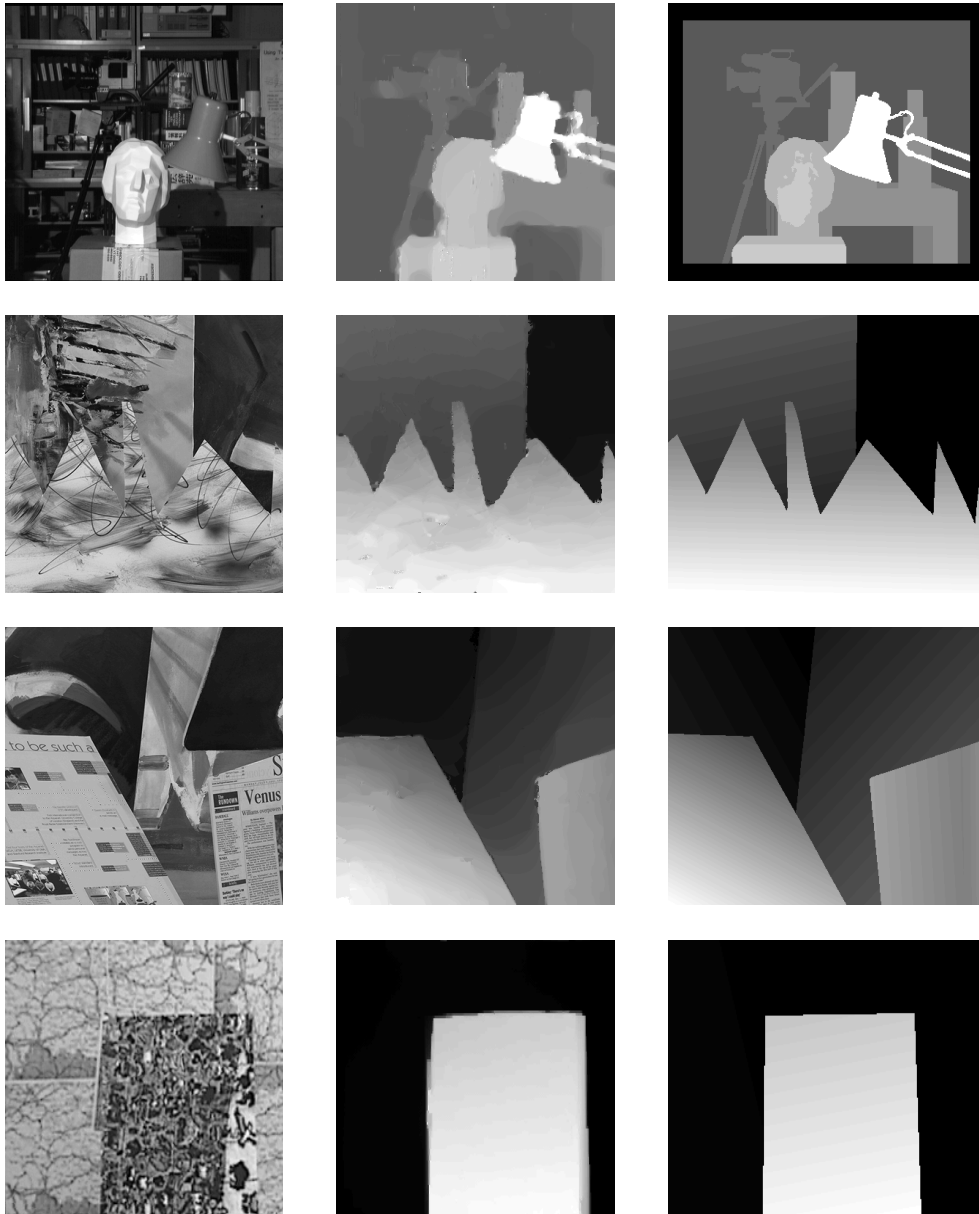


Figure 3. Results on Middlebury data set. From top to bottom: Tsukuba, Sawtooth, Venus, Map. From left to right: Reference images, extracted disparity maps and ground truth disparity maps.

| Technique | Tsukuba | Sawtooth | Venus | Map |
|---------------------------------|-------------|-------------|-------------|-------------|
| Prop.Meth. $(\cap_{i=1}^3 S_i)$ | 0.29 | 0.23 | 0.24 | 0.35 |
| Prop.Meth. $(S_2 \cap S_3)$ | 0.46 | 0.31 | 0.45 | 0.49 |
| Prop.Meth. $(S_1 \cap S_2)$ | 0.37 | 0.27 | 0.28 | 0.43 |

Table 2. AADE comparison of our results on Middlebury database.

- [2] A. Fusiello, V. Roberto, and E. Trucco. Symmetric stereo with multiple windowing. *Int. Journal of Pattern Recognition and Artificial Intelligence*, 14(8):1053–1066, 2000.
- [3] C. L. Zitnick and T. Kanade. A cooperative algorithm for stereo matching and occlusion detection. *IEEE Trans. Pattern Anal. Machine Intell.*, 22(7):675–684, July 2000.
- [4] M. Agrawal and L. Davis. Window-based, discontinuity preserving stereo. *Proc. IEEE Computer Vision and Pattern Recognition (CVPR)*, 2004.
- [5] D. Scharstein and R. Szeliski. A taxonomy and evaluation of dense two-frame stereo correspondence algorithms. *Int. Journal of Computer vision*, 47(1):7–42, 2002.
- [6] G. Aubert, R. Deriche, and P. Kornprobst. Computing optical flow via variational techniques. *SIAM Journal on Numerical Analysis*, pages 156–182, 1999.
- [7] L. Alvarez, R. Deriche, J. Sanchez, and J. Weickert. Dense disparity map estimation respecting image discontinuities: A pde and scale-space based approach. *Journal of Visual Communication and Image Representation*, 13:3–21, 2002.
- [8] N. Slesareva, A. Bruhn, and J. Weickert. Optic flow goes stereo: A variational method for estimating discontinuity-preserving dense disparity maps. *Pattern Recognition*, pages 33–40, 2005.
- [9] P.Y. Simard and G.E. Mailloux. Vector field restoration by the method of convex projections. *Computer Vision, Graphics, and Image Processing*, June 2000.
- [10] P.L. Combettes. The convex feasibility problem in image recovery. *Advances in Imaging and Electron Physics*, 95:155–270, 1996.
- [11] L.I. Rudin, S. Osher, and E. Fatemi. Nonlinear total variation based noise removal algorithms. *Physica D*, 60:259–268, 1992.
- [12] A. Fusiello, E. Trucco, and A. Verri. A compact algorithm for rectification of stereo pairs. *Machine Vision and Applications*, 12(1):16–22, 2000.
- [13] P.L. Combettes. A block iterative surrogate constraint splitting method for quadratic signal recovery. *IEEE Trans. Signal Proc.*, 51(7):1771–1782, July 1997.
- [14] E. Geoffrey and P.W. Richard. Detecting binocular half-occlusions: Empirical comparisons of five approaches. *IEEE Trans. Pattern Anal. Machine Intell.*, 42(8):1127–1133, August 2002.
- [15] S. Osher and N. Paragios. *Geometric Level Set Methods in Imaging, Vision and Graphics*. Springer Verlag, 2003.
- [16] P.L. Combettes and J.C. Pesquet. Image restoration subject to a total variation constraint. *IEEE Trans. Image Proc.*, 13(9):1213–1222, 2004.
- [17] H.H. Nagel and W. Enkelmann. An investigation of smoothness constraints for the estimation of displacement vector fields from image sequences. *IEEE Trans. on Pattern Anal. Mach. Intell.*, 8:565–593, 1986.
- [18] M. Bleyer and M. Gelautz. A layered stereo algorithm using image segmentation and global visibility constraints. *Int. Conf. Image Proc.*, pages 2997–3000, 2004.
- [19] M. Bleyer and M. Gelautz. Graph-based surface reconstruction from stereo pairs using image segmentation. *Videometrics VIII, SPIE-5665:288–299*, 2005.
- [20] C. Kim, K.M. Lee, B.T. Choi, and S.U. Lee. A dense stereo matching using two-pass dynamic programming with generalized ground control points. *Computer Vision and Pattern Recognition*, 2:1075–1082, 2005.
- [21] Y. Deng, Q. Yang, X. Lin, and X. Tang. A symmetric patch-based correspondence model for occlusion handling. *Int. Conf on Computer Vision*, 2:1316–1322, 2005.